PCCP

Accepted Manuscript

ROYAL SOCIETY OF CHEMISTRY

www.rsc.org/pccp

Isomer-selective infrared spectroscopy of the cationic trimethylamine dimer to reveal its charge sharing and enhanced acidity of the methyl groups

Yoshiyuki Matsuda [a,b]*, Yuichiro Nakayama [a], Naohiko Mikami [a], and Asuka Fujii [a]*

[a] Department of Chemistry, Graduate School of Science, Tohoku University, Aramaki-Aoba 6-3, Aoba-ku, Sendai, 980-8578, Japan

E-mail: matsuda@ m.tohoku.ac.jp and asukafujii@m.tohoku.ac.jp

[b] Center for the Advancement of Higher Education, Tohoku University, Kawauchi 41, Aoba-ku, Sendai, 980-8576, Japan

Infrared predissociation spectroscopy of the trimethylamine dimer cation generated by the vacuum-ultraviolet photoionization is isomer-selectively carried out by monitoring two main fragment channels, protonated trimethylamine and trimethylamine monomer cation. The spectral carriers monitored by these two channels are assigned to different isomers of the trimethylamine dimer cation. One is the charge-shared (hemibond) structure, in which the positive charge is intermolecularly delocalized over the dimer through the interaction between the nonbonding orbitals of the nitrogen atoms. In the other isomer, a proton of a methyl group in the ionized moiety is intermolecularly transferred to the nitrogen atom of the neutral moiety and is shared between the carbon and nitrogen atoms. The latter isomer shows that the methyl groups of cationic trimethylamine are highly acidic. This example demonstrates characteristic properties of radical cations with alkyl groups.

INTRODUCTION

Radical cations are often generated in various chemical and physical processes such as ion-molecule reactions of interstellar and atmospheric systems,[1, 2] electrolytic reactions of conducting polymers,[3, 4] ionization in mass spectrometry,[5] and radiation-induced dynamics.[6] They are generally highly reactive so that they would play crucial roles to drive these processes. Therefore, precise understanding of their properties and reactivity would be one of key issues to microscopically understand these processes. However, their short lifetimes in bulk systems due to their high reactivity and unstability impede investigations on their detailed properties.

The collision-free condition in a supersonic jet expansion is ideal to perform spectroscopic investigation of radical cations and their clusters because they can have long lifetimes by elimination of collisional reactions.[7-10] Recently, the IR spectroscopic investigations have been reported for the unstable radical cluster cations of ammonia, alcohols, and acids which were generated by vacuum-ultraviolet photoionization.[11,12] The water cluster cations, which are generated by the electron ionization combined with efficient cooling by a high pressure jet expansion, have also been investigated by IR spectroscopy.[13,14] These studies have demonstrated that these cluster cations form the proton-transferred structures, where the proton of OH or NH of the ionized moiety is transferred to the neutral moiety so that the protonated moiety and the neural deprotonated radical are bound. The theoretical simulations at the various levels have indicated these intermolecular proton transfer reactions occur without an effective energy barrier after ionization.[11-13,15-20] These results demonstrate that OH and NH of radical cations are highly acidic.

Acidities of CH bonds are generally very low, and CH bonds are regarded as a nonpolar functional group, which is basically inert and has no strong intermolecular interactions such as a hydrogen bond, although weak interactions between CH and π electron clouds or nonbonding electrons and their chemical importance have frequently been discussed.[21-23] Therefore, we ordinarily consider that the role of CH in intra- and intermolecular structures is practically limited to the origin of the steric effects and dispersion force. Moreover, proton transfer from CH bonds is ordinarily ignored. However, similar to OH and NH of radical cations of protic molecules,[11-20] enhancements of acidities of CH would be expected in positively-charged systems. This expectation implies that such acidic CH plays significant roles in structure determination and also acts as a proton source in chemical processes. Though various proton transfer products from CH have been suggested by mass spectrometry of many ionization processes,[24-29] spectroscopic confirmation of the enhanced acidity of cationic CH has rarely been reported. The observation of the enhanced infrared intensity of CH stretch bands has been reported for several radical cations.[30, 31] These intensity enhancements of the CH stretch bands may imply the high acidities of their CH bonds. To investigate enhancements of acidities of cationic CH, interactions of cationic CH with proton acceptor molecules should be addressed. However, no direct experimental observation of such a cationic CH bond bound to an acceptor has been reported.

For the radical cluster cations of protic molecules, the charge-shared (hemibond) structures have also been theoretically proposed as the stable structures.[11,13,15-20] In such a structure, the positive charge is shared in the cluster through the interactions between the nonbonding orbitals. The shared charge is not localized at the lone pairs

but it delocalizes into the whole body of the molecules. For such charge-shared structures of cluster cations of protic molecules, firm experimental evidence has not been reported because they are less stable than proton-transferred structures. On the other hand, the charge-shared structures have been reported for the cluster cations of aromatic systems as well as small molecular systems such as CO, CO_2, NO, and NO_2.[32-35] In these systems, the charge is accommodated by intermolecular interactions among π orbitals and/or nonbonding orbitals, and delocalizes throughout the molecules in the clusters through their π orbitals.

In this study, we report an infrared (IR) spectroscopic investigation of the geometric structure of the trimethylamine (TMA) dimer cation. Two different IR predissociation spectra of $(TMA)_2^+$ are observed by monitoring the different fragment mass channels of TMA^+ and H^+TMA. They shows different spectral features, which are assigned to different isomers. Comparisons of the IR spectra with quantum chemical calculations of energies, structures, and harmonic vibrational simulations reveal that $(TMA)_2^+$ forms two isomeric structures of the charge-shared structure between the nitrogen atoms and the proton-transferred structures from CH to the nitrogen atom. The charge-shared structure of $(TMA)_2^+$ experimentally demonstrates the formation of such a structure of saturated organic molecules for the first time. Furthermore, the C···HN interaction formed in the proton-transferred structure is a new type of the intermolecular interaction. The C···HN type proton-transferred structure substantiates the strong acidity of the cationic CH bond.

EXPERIMENTS AND CALCULTATIONS

Infrared (IR) spectra of $(TMA)_2^+$ as well as neutral $(TMA)_2$ were observed by the IR predissociation spectroscopy based on the vacuum-ultraviolet (VUV) photoionization detection.[36] The spectroscopic schemes are called VUV-ionization detection-IR predissociation spectroscopy (VUV-ID-IRPDS) for the neutral and IR predissociation spectroscopy of VUV-pumped ion (IRPDS-VUV-PI) for the cation.[36] In this study, the VUV light at 118 nm was used.

In VUV-ID-IRPDS for $(TMA)_2$, the ion intensity of $(TMA)_2^+$, which was generated by the VUV photoionization, was size-selectively monitored with the time-of-flight mass spectrometer. The IR light was introduced prior to the VUV photoionization and its frequency was scanned. The vibrational absorptions of $(TMA)_2$ were detected as decrease of the monitored ion intensity through the vibrational predissociation following the vibrational transitions of $(TMA)_2$.

To perform IRPDS-VUV-PI for $(TMA)_2^+$, the tandem-type quadrupole mass spectrometer (Q-mass) was used. The $(TMA)_2^+$ cation was generated by the VUV photoionization of the neutral dimer in a supersonic jet. The IR light irradiated the size-selected $(TMA)_2^+$ cation after the first Q-mass. Fragment ions originating from the vibrational predissociation of $(TMA)_2^+$ were size-selectively detected by the 2nd Q-mass. Thus, a size-selective IR spectrum of $(TMA)_2^+$ was observed as an enhancement spectrum by monitoring the TMA cation or protonated TMA fragment mass channels.

Optimized structures, harmonic vibrations, atomic charges, potential curves in proton-transfer coordinates were calculated with the GAUSSIAN 09 program package

and the attached GAUSSIAN NBO Version 3.1.[37] Optimized structures are visualized with the MOLEKEL program.[38]

RESULTS AND DISCUSSION

Fig.1(a) presents the IR spectrum of neutral $(TMA)_2$ measured by VUV-ID-IRPDS. The 118 nm VUV light was used for ionization and the $(TMA)_2^+$ mass channel was monitored. The neutral dimer is the precursor for the generation of $(TMA)_2^+$ by the photoionization at 118 nm. The simulated IR spectrum based on the optimized structure at the ωB97X-D/6-311++G(3df, 3dp) level is also shown in the figure. This structure is the most stable one at the M06/6-311++(2d,2f), PBE1PBE/6-311++(2d,2f), and MP2/6-311++G(d, p) levels. The simulated spectrum reproduces the overall feature of the observed spectrum, although there exist some minor discrepancies because of the anharmonic coupling. Fig.1(b) shows the mass spectrum of the fragment ions in the spontaneous dissociation of the TMA dimer cation in the photoionization process at 118 nm. The spectrum was observed with a tandem-type Q-mass spectrometer by scanning the second Q-mass filter while the first filter is tuned to select only the TMA dimer cation. Protonated TMA (H^+TMA) as well as the TMA cation (TMA^+) are observed as the main fragments in the spontaneous dissociation of $(TMA)_2^+$. The production of protonated TMA clusters has been seen in the mass spectrometric studies of TMA.[26, 27] The production of H^+TMA from $(TMA)_2^+$ can be explained by the intracluster proton-transfer from the methyl group and following dissociation.

Figs.2(a) and (b) show the observed IR predissociation spectra of $(TMA)_2^+$ by monitoring the fragment channels of (a) TMA^+ and (b) H^+TMA, respectively. $(TMA)_2^+$

was generated with the photoionization of the neutral dimer at 118 nm, which ejects the nonbonding electron of the nitrogen atom.[39] In observed spectrum (a), there appears only the CH stretch bands at 2800~3100 cm^{-1}. In observed spectrum (b), in addition to the CH stretch band at 2990 cm^{-1}, an extraordinarily broad feature appears below 2800 cm^{-1} and its frequency is obviously lower than the typical alkyl CH stretch frequency (2800-3000 cm^{-1}). A broad absorption in this frequency range (< 2800 cm^{-1}) is a typical feature of the stretch vibration of a proton which is shared by two atoms through a strong hydrogen bond (so-called proton vibration).[7, 11-14] The band broadening is attributed to contributions of hot bands because of high internal temperature as well as the enlargements of anharmonic couplings of the donor XH stretch by the hydrogen bond formation.[40]

Figs.2(c)-(e) are the calculated IR spectra based on the optimized structures at the ωB97X-D/6-311++G(3df,3dp) level. Three stable structures were found at this level. These three optimized structures of the N···N, C···HN, and N···HN types are depicted in Figs.3(a)-(c), respectively. The stable isomeric structures and their relative energies obtained at other calculational levels are summarized in the electronic supplementary information. In structure (a) of the N···N type, the positive charge is shared through the intermolecular interaction between the nonbonding orbitals of the nitrogen atoms (labeled by N1 and N2). In structure (b) of the C···HN type, the proton H4 is shared by the N2 and C3 atoms. On the other hand, the H4 proton is shared between the N1 and N2 atoms in structure (c) of the N···HN type. Both of structures (b) and (c) can be formed through the intermolecular proton transfer from the methyl group of the ionized TMA moiety.

Because the N···N type structure does not have a shared proton, only the free CH stretch bands appear in simulated spectrum (c) at the frequency range of 2100-3650 cm^{-1}. This spectral feature agrees well with observed spectrum (a). We therefore conclude that spectrum (a) is attributed to the charge-shared structure in Fig.3(a). As shown in Fig.3, the two other types of isomers of $(TMA)_2^+$, structures (b) and (c), have a shared proton (labeled by H4 in Fig.3). The C···HN type is more stable than the N···HN type at all the calculation levels (ωD97-XD/6-311++G(3pd,3df), M06-2X/6-311++G(2d,2p), and PBE1PBE with the 6-311++G(2d,2p), 6-31++G**, and 6-31+G* basis sets). In addition, upon the ionization process of the neutral dimer, the N···HN type structure ought to be formed through the C···HN type structure from the neutral geometry. It is, therefore, reasonable to assume that the C···HN type structure is dominantly formed in these two proton-shared structures. This is supported by the fact that the simulated NH frequency of the C···HN type shows better agreement with the observed broad band. Therefore, we conclude that the major carrier of observed spectrum (b) is the C···HN type structure (structure (b) in Fig.3). Contribution of the coexisting N···HN isomer is not excluded because overlap of the spectra at both the regular CH stretch band and the shared proton band cannot be distinguished from the pure spectrum of the C···HN type structure.

In conclusion, the spectral carriers of observed spectra (a) and (b) in Fig.2 are assigned to the N···N and C···HN types, respectively. Thus, $(TMA)_2^+$ forms the two different type structures, of which energy difference is estimated to be ~1 kcal/mol by the several DFT calculations. Spectrum (a) is the IR predissociation spectrum observed by

monitoring the TMA^+ mass channel, while spectrum (b) was observed by monitoring the H^+TMA mass channel. The clear dependence on the monitoring channel indicates that the two isomers of $(TMA)_2^+$ dissociate to the different fragment channels, respectively. In IR predissociation processes of molecular clusters, intermolecular bonds are dominantly cleaved because their binding energies are much lower than those of covalent bonds. In the IR predissociation process of the N···N type structure, the N···N bond (hemibond) would be broken. Thus, the N···N type isomer preferentially dissociates to the TMA cation and neutral TMA without further isomerization. Similarly, because the C···HN type dissociates to H^+TMA and dehydrated TMA radical by cleavage of the C···HN bond. As an example of similar isomer-separation of IR spectra by monitoring different fragment channels, the case of protonated 3-cyanophenylalanine-TMA has been reported very recently.[41] In this case, however, isomer separation of the spectra was not perfect, suggesting contributions of common spectral carriers and/or isomerization after the IR excitation. In the present case, the number of the stable isomers is small and the isomerization between the N···N type and the C···HN type would not be plausible. Therefore, spectra (a) and (b) in Fig.2 were isomer-selectively observed by monitoring the TMA^+ and H^+TMA channels, respectively.

The N···N type isomer has the D_{3h} symmetry and the two molecules in the cluster shares the positive charge through the N···N interaction. Table 1 lists the atomic charges of neutral TMA, cationic TMA^+, and the N···N type isomer of $(TMA)_2^+$. The atomic charges are calculated by the natural bond orbital (NBO) analysis at the ωB97X-D/6-311++G(3df,3dp) level. All the atomic charges of $(TMA)_2^+$ are intermediate values

between those of neutral and cationic TMA^+. The NBO analysis demonstrates that the positive charge is equally shared by each TMA molecule in the dimer (the excess positive charge of 0.5 a.u. is in each unit). The atomic charges listed in Table 1 indicate the delocalization of the positive charge over all the atoms in $(TMA)_2^+$. This charge delocalization stabilizes the N···N type structure by 23.8 kcal/mol at ωB97X-D/6-311++G(3df,3dp). This stabilization energy is equivalent to the binding energy of the hemibond.

The charge delocalization through the intermolecular charge sharing has been theoretically predicted for the dimer cations of water, ammonia, and so on, which are composed by the atom in the first and second periods. [11,13,15-20] However, no firm observation of the charge delocalized structures has been reported for these molecules because they have more stable isomers. The present observation of the N···N type structure of $(TMA)_2^+$ is the first experimental demonstration of intermolecular charge sharing as well as charge delocalization in molecular clusters without π orbitals.

In the C···HN type structure, the proton is transferred from the methyl group and is shared between the carbon and nitrogen atoms. This C···HN type interaction is rare and it cannot be categorized into the typical hydrogen bond because the proton of the NH bond is bound to the hole of the singly occupied molecular orbital (SOMO) of the neutral radical site. The covalent interaction would largely contribute to this C···HN interaction. This type of structures and interactions, where a proton is shared between a carbon atom and an electronegative atom such as nitrogen atom, is experimentally identified for the first time, to the best of our knowledge. To examine the potential landscape of the proton-transfer route from the methyl group to form the C···HN type

structure, the energy along the intermolecular proton-transfer coordinate is calculated by changing the C1–H2 distance from the C···HN type structure while optimizing all the other structural parameters. The calculated potential energy curve at the ωB97X-D/6-311++G(3df,3dp) level is shown in Fig.4. As seen in the figure, the proton of the methyl group of the cationic moiety is transferred to the N atom of the neutral moiety without an effective energy barrier. This barrierless transfer of the methyl proton as well as the formation of the C···HN type structure concretely demonstrates the high acidity of the methyl group of the TMA cation. The observation of the stretch band of the shared proton experimentally substantiates the large enhancement of the acidity of the TMA^+ moiety in $(TMA)_2^+$ and this assures the calculations. Although it is difficult in the gas phase to define an acidity based on chemical equilibrium, the single minimum potential curve in the proton transfer coordinate indicates that TMA^+ acts as the Bronsted acid with neutral TMA. Thus, the TMA cation is highly protic although its neutral is obviously aprotic. The formation energy of the C···HN type structure from neutral and cationic monomers is calculated to be 22.8 and 22.5 kcal/mol at the ωB97X-D/6-311++G(3df,3dp) and M06-2X/6-311++G(2d,2p) levels, respectively. Very recently, a theoretical investigation has been made for structures and binding energies of the closed shell cations of trimethylsulfide and tetramethylamine with N-methylacetamide with the MP2 level ab-initio and DFT calculations.[42] They also showed the enhancement of the proton donor abilities in the CH···O interactions, although these clusters prefer the multifurcating structures where plural CH bonds of the cationic moiety simultaneously act as the proton donors to the oxygen atom of N-methylacetamide. The C···HN binding energy of the open shell $(TMA)_2^+$ cation is even larger than the binding energies

of these multifurcating structures. The binding energy of the C···HN type structure is much higher than those of typical neutral hydrogen-bonds [24, 43] and is close to the binding energies of cationic clusters of protic molecules, such as water, ammonia, alcohols, and acids.[7, 11-13, 24] The C···HN hydrogen bond is obviously categorized into a strong hydrogen bond.

CONCLUSION

In this study, the IR spectra of $(TMA)_2^+$ generated with the VUV photoionization was isomer-selectively observed by monitoring the different fragment mass channels. Ionized $(TMA)_2$ isomerizes to the two stable cationic structures of the N···N and C···HN types, which are formed by the characteristic intermolecular interactions, respectively.

In the N···N type structure, the positive charge is equally shared by the intermolecular interaction of the nonbonding orbitals of the two nitrogen atoms. The charge delocalizes throughout each TMA unit in the cluster. This observation indicates that the positive charge can delocalize inter- and intra-molecularly in the molecular systems without π orbitals. Namely, this supports the possibility of formations of charge-shared structures in molecular systems such as water, alcohols, amines, acids, and so on, although no firm observation has been made for them. Therefore, charge sharing should be counted for various chemical processes, where radical cations are often generated.

In the C···HN type structure, the proton of the methyl group is transferred and is intermolecularly shared by the carbon and nitrogen atoms. The potential energy curve

along the proton transfer path shows that the proton is transferred without an effective energy barrier. This is concrete demonstration of the high acidity of the methyl group of cationic TMA. Numberless CH bonds ubiquitously exist in chemical, biological, environmental, and astrochemical systems, and some of them involve charged moieties. The high acidity of the methyl group in the TMA cation was shown in this study. This result implies that such a positively charged CH bond can form a strong hydrogen bond and be an important factor of molecular and intermolecular conformational preferences, molecular reactivity, and functions of biomolecular systems. To understand their properties at the molecular level, we would like to emphasize the necessity of taking the special property of cationic CH bonds into account properly.

References

1 E.E. Feerguson, *Ann. Rev. Phys. Chem*. 1975, **26**, 17-38.

2 P. S. Monks, *Chem. Soc. Rev*. 2005, **34**, 376–395.

3 G. Odian, *Principles of Polymerization* (4th ed.). Wiley Interscience, 2004.

4 R. J. Waltman, J. Bargon, *Can. J. Chem.* 1986, **64**, 76-95.

5 E. de Hoffmannnn, V. Stroobant, *Mass Spectrometry: Principles and Applications (3rd ed.)*, John Wiley & Sons, 2007.

6 I. G. Draganic, Z. D. Draganic, *The Radiation Chemistry of Water*, ACADEMIC PRESS, 1971.

7 J. M. Lisy, *J. Chem. Phys.* 2006, **125**, 132302-1-19.

8 T. A. Miller, *Science*, 1984, **10**, 545-553.

9 J. M. Hollas, D. Phillips, *Jet Spectroscopy and Molecular Dynamics*, Springer, 1994.

10 B. Brutschy, *Chem. Rev.* 1992, **92**, 1567-1587.

11 M. Hachiya, Y. Matsuda, K. Suhara, N. Mikami, A. Fujii, *J. Chem. Phys.* 2008, **129**, 094306-1-8.

12 K. Ohta, Y. Matsuda, N. Mikami, A. Fujii, *J. Chem. Phys.* 2009, **131**, 184304-1-11.

13 G. H. Gardenier, M. A. Johnson, A. B. McCoy, *J Phys. Chem.* 2009, **113**, 4772-4779.

14 K. Mizuse, J. L. Kuo, A. Fujii, *Chem. Sci.* 2011, **2**, 868-876.

15 P. M. W. Gill, L. Radom, *J. Am. Chem. Soc.* 1988, **110**, 4931-4941.

16 M. Sodupe, J. Bertran, L. Rodríguez-Santiago, E. J. Baerends, *J. Phys. Chem. A*, **1999**, 103, 166-170.

17. H. M. Lee, K. S. Kim, *J. Chem. Theory Comupt.* **2009**, 5, 976-981.

18 Q. Cheng, F. A. Evangelista, A. C. Simmonett, Y. Yamaguchi, H. F. Schaefer, III, *J. Phys. Chem. A*, **2009**, 113, 13779-13789.

19 P. -P. Pan, Y. -S. Lin, M. -K. Tsai, J. -L. Kuo, J. -D. Chai, *Phys. Chem. Chem. Phys* . 2012, **14**, 10705–10712.

20 M. -K. Tsai, J. -L. Kuo, J. -M. Lucd, *Phys. Chem. Chem. Phys.* 2012, **14**, 13402–13408.

21 S. Scheiner, *Phys. Chem. Chem. Phys.* 2011, **13**, 13860-13872.

22 M. Nishio, *Phys. Chem. Chem. Phys.*, 2011, **13**, 13873-13900.

23 G. R. Desiraju, *Angew. Chem. Int. Ed.* 2011, **50**, 52-59.

24 M. Meot-Ner, (Mautner), *Chem. Rev.* 2012, **112**, PR22-PR103.

25 J. F. Garvey, W. R. Peifer, M. T. Coolbaugh, *Acc. Chem. Res.* 1991, **24**, 48-54.

26 S. Wei, W. B. Tzeng, A. W. Castleman, Jr., *J. Phys. Chem.* 1991, ***95***, 585-591.

27 W. B. Tzeng, K. Narayanan, G. C. Chang, W. C. Tsai, J. J. Ho, *J. Phys. Chem*. 1996, **100**, 15340-15345.

28 Y. Matsuda, K. Hoki, S. Maeda, K. Hanaue, K. Ohta, K. Morokuma, N. Mikami, A. Fujii, *Phys. Chem. Chem. Phys.* 2012, **14**, 712-719.

29 A. Golan, K. B. Bravaya, R. Kudirka, O. Kostko, S. R. Leone, *Nature Chem.* 2012, **4**, 323-329.

30 A. Fujii, E. Fujimaki, T. Ebata, N. Mikami, *J. Chem. Phys.* 2000, **112**, 6275-6284.

31 G. E. Douberly, A. M. Ricks, B. W. Ticknor, P. v. R. Schleyer, M. A. Duncan, *J. Am. Chem. Soc.* 2007, **129**, 13782-13783.

32 Y. Xie, W. Wang, K. Fan, H. F. Schaefer, *J. Chem. Phys.* 2002, **117**, 9727-9732.

33 Y. Inokuchi, A. Muraoka, T. Nagata, T. Ebata, *J. Chem. Phys.* 2008, **129**, 044308-1-9.

34 Y. Inokuchi, R. Matsushima, Y. Kobayashi, T. Ebata, *J. Chem. Phys.* 2009, **131**, 044325-1-6.

35 P. A. Pieniazek, S. E. Bradforth, A. I. Krylov, *J. Chem. Phys.* 2008, **129**, 074104-1-11.

36 Y. Matsuda, N. Mikami, A. Fujii, *Phys. Chem. Chem. Phys.* 2009, **11**, 1279-1290.

37 Theoretical calculations were carried out with the Gaussian 09 program package. *Gaussian 09, Revision A.02*, M. J. Frisch, G. W. Trucks, H. B. Schlegel, G. E. Scuseria, M. A. Robb, J. R. Cheeseman, G. Scalmani, V. Barone, B. Mennucci, G. A. Petersson, H. Nakatsuji, M. Caricato, X. Li, H. P. Hratchian, A. F. Izmaylov, J. Bloino, G. Zheng, J. L. Sonnenberg, M. Hada, M. Ehara, K. Toyota, R. Fukuda, J. Hasegawa, M. Ishida, T. Nakajima, Y. Honda, O. Kitao, H. Nakai, T. Vreven, J. A. Montgomery, Jr., J. E. Peralta, F. Ogliaro, M. Bearpark, J. J. Heyd, E. Brothers, K. N. Kudin, V. N. Staroverov, R. Kobayashi, J. Normand, K. Raghavachari, A. Rendell, J. C. Burant, S. S. Iyengar, J. Tomasi, M. Cossi, N. Rega, J. M. Millam, M. Klene, J. E. Knox, J. B. Cross, V. Bakken, C. Adamo, J. Jaramillo, R. Gomperts, R. E. Stratmann, O. Yazyev, A. J. Austin, R. Cammi, C. Pomelli, J. W. Ochterski, R. L. Martin, K. Morokuma, V. G. Zakrzewski, G. A. Voth, P. Salvador, J. J. Dannenberg, S. Dapprich, A. D. Daniels, Ö. Farkas, J. B. Foresman, J. V. Ortiz, J. Cioslowski, and D. J. Fox, Gaussian, Inc., Wallingford CT, 2009.

38 Flukiger, P.; Luthi, H. P.; Portmann, S.; Weber, J.; *Molekel 4.0*, Swiss Center for Scientific Computing, Manno, Switzerland, 2000.

39 K. Kimura, K. Osafune, *Mol. Phys.* 1975, **29**, 1073-1083.

40 T. Yamashita, K. Takatsuka, *J. Chem. Phys.* **2007**, 126, 074304-1-15

41 W. S. Hopkins, R. A. Marta, T. B. McMahon, *J. Phys. Chem. A*, 2013, **117**, 10714-10718.

42 S. Scheiner, U. Adhikari, *J. Phys. Chem. A*, 2013, **117**, 10551-10562.

43 a) L. Pauling, *The Nature of the Chemical Bond*, Cornell, 1939; b) G. A. Jeffrey, *An Introduction to Hydrogen Bonding*, Oxford, 1997; c) G. Gilli, P. Gilli, *The Nature of the Hydrogen Bond*, Oxford, 2009.

Acknowledgement

We thank Dr. T. Maeyama for his helpful discussion. Y.M. acknowledges the financial support by the Sumitomo Foundation (111365).

Table 1 Natural atomic charges in the atomic units of TMA, TMA^+, and $(TMA)_2^+$ at the ωB97X-D/6-311++G(3df,3dp) level

TMA		TMA^+		$(TMA)_2^+$	
Atom	Atomic charge	Atom	Atomic charge	Atom	Atomic charge
N	-0.56	N	-0.04	N	-0.31
C	-0.35	C	-0.41	C	-0.38
H	0.19 [a)]	H	0.24~0.26 [c)]	H	0.21~0.22 [c)]
	0.16 [b)]				

a) Atomic charge of two hydrogen atoms in each methyl group

b) Atomic charge of one hydrogen atom in each methyl group

c) Atomic charges of hydrogen atoms are within the listed values.

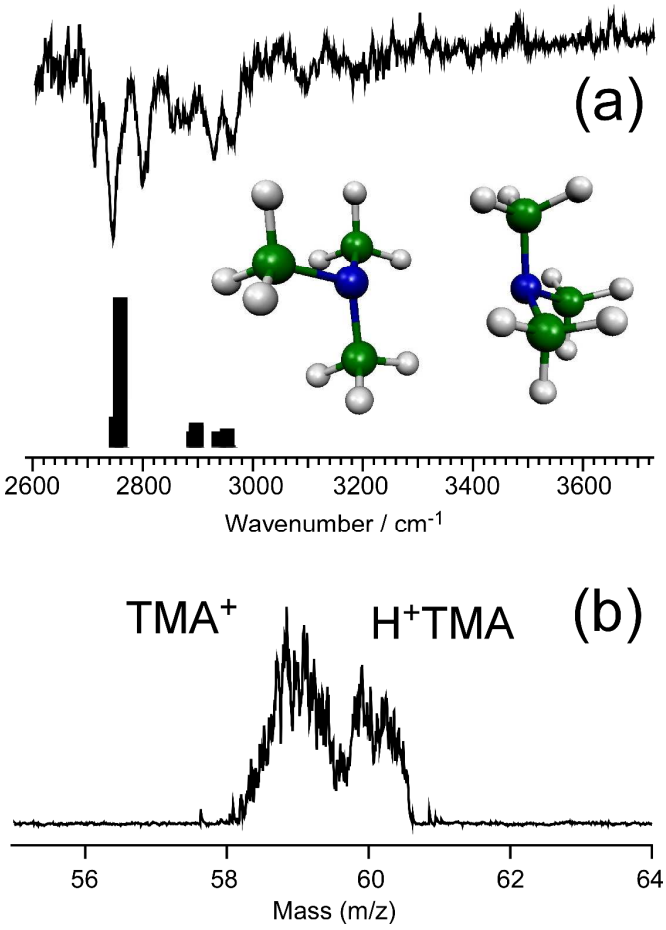

Fig. 1 (a) The observed infrared spectrum of the neutral trimethylamine (TMA) dimer with VUV-ID-IRPDS by monitoring the TMA dimer cation mass channel. The calculated spectrum based on the most stable optimized structure at the ωB97X-D/6-311++G(3df,3dp) level is also shown. The structure is depicted as the inset. (b) The mass spectrum of the fragment cations in the spontaneous dissociation of the photo-ionized TMA dimer at 118 nm. The spectrum was observed by the tandem type Q-mass filters. The first Q-mass was fixed to pass only the TMA dimer cation and the second Q-mass filter was scanned.

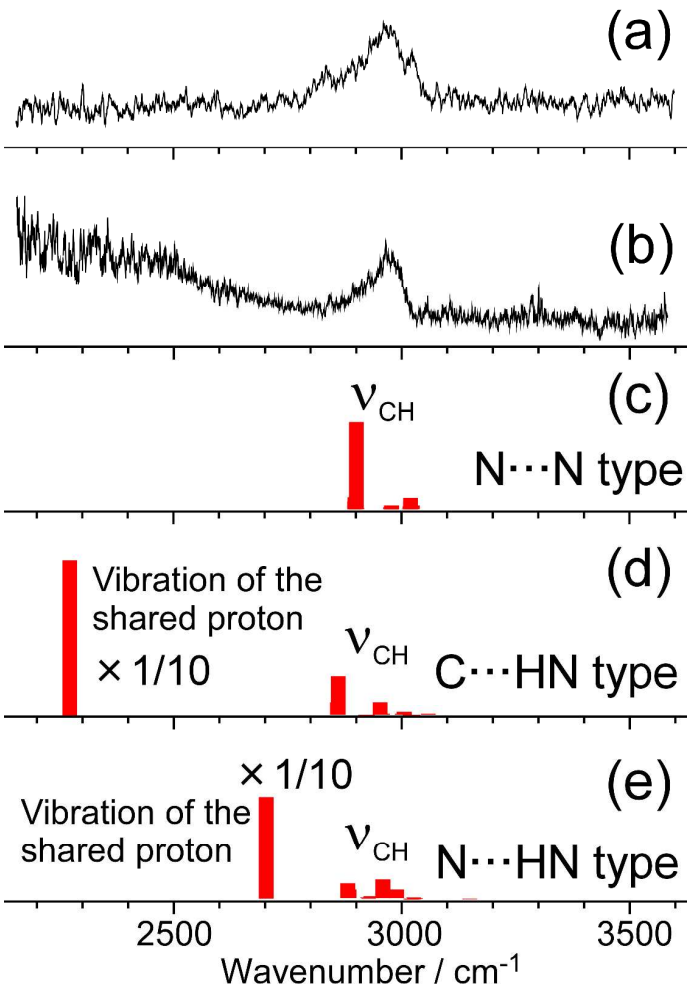

Fig. 2 (a), (b) The observed infrared spectra of the TMA dimer cation and (c-e) the calculated spectra based on its optimized structures at the ωB97X-D/6-311++G(3df,3dp) level. Spectra (a) and (b) were measured by IR predissociation spectroscopy with monitoring the TMA^+ and H^+TMA mass channels, respectively. The intensities of spectra (a) and (b) are normalized by the IR power. Calculated spectra (c), (d), and (e) are simulated based on optimized structures (a), (b), and (c), depicted in Fig. 3, respectively. The calculated spectra are scaled by the factor of 0.97 .

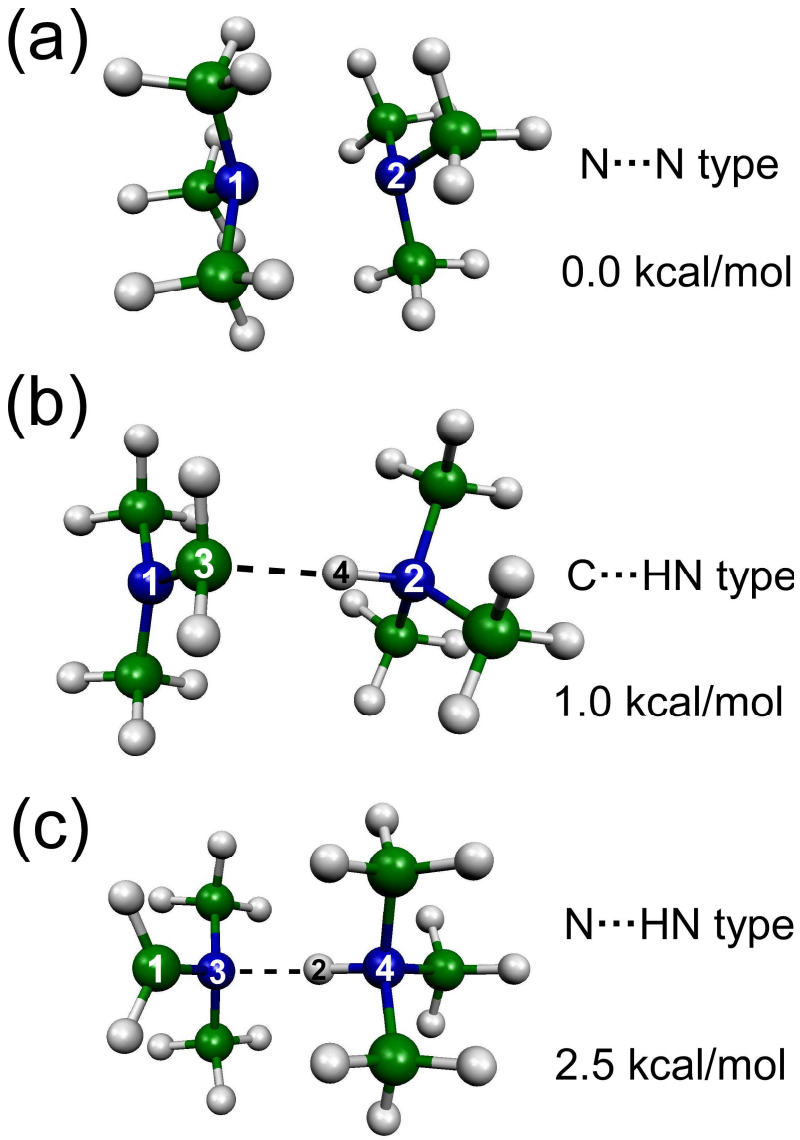

Fig. 3 Optimized structures of the TMA dimer cation at the ωB97X-D/6-311++G(3df,3dp) level. The relative energies shown in the figure are corrected by the zero-point energies.

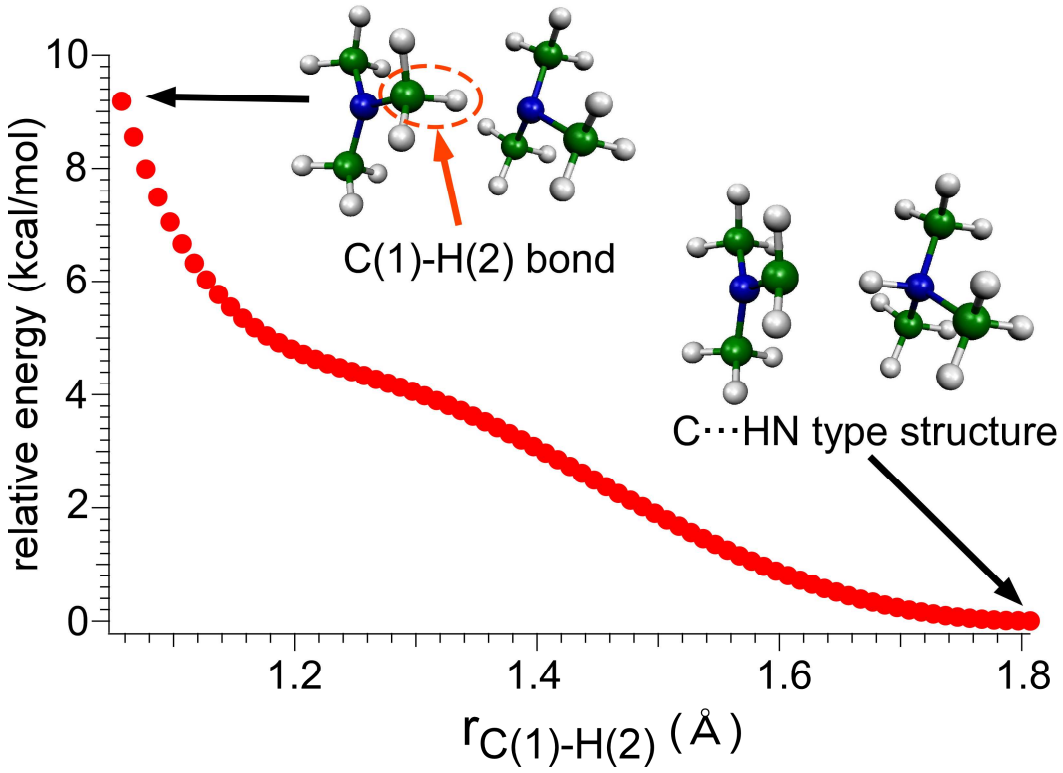

Fig. 4 Potential energy curve along the proton-transfer reaction coordinate of the TMA dimer cation. The potential energies were calculated at the ωB97X-D/6-311++G(3df,3dp) level by fixing the CH distance (R_{CH}) of the transferred proton while optimizing all the other structural parameters.

Table of Contents Entry

The isomer-selective infrared spectroscopy revealed the charged-shared (hemi bond) and the C···HN hydrogen-bond structures of the trimethylamine dimer cation.